nature climate change

SUPPLEMENTARY INFORMATION

https://doi.org/10.1038/s41558-020-0776-2

In the format provided by the authors and unedited.

Decreased motility of flagellated microalgae long-term acclimated to CO_2-induced acidified waters

Yitao Wang[1,2], Xiao Fan[1], Guang Gao[3], John Beardall[3,4], Kazuo Inaba[5], Jason M. Hall-Spencer[5,6], Dong Xu[1], Xiaowen Zhang[1], Wentao Han[1], Andrew McMinn[7] and Naihao Ye[1,2] ✉

[1]Yellow Sea Fisheries Research Institute, Chinese Academy of Fishery Sciences, Qingdao, China. [2]Function Laboratory for Marine Fisheries Science and Food Production Processes, Qingdao National Laboratory for Marine Science and Technology, Qingdao, China. [3]State Key Laboratory of Marine Environmental Science & College of Ocean and Earth Sciences, Xiamen University, Xiamen, China. [4]School of Biological Sciences, Monash University, Clayton, Victoria, Australia. [5]Shimoda Marine Research Center, University of Tsukuba, Shizuoka, Japan. [6]School of Biological and Marine Sciences, University of Plymouth, Plymouth, UK. [7]Institute of Antarctic and Southern Ocean Studies, University of Tasmania, Tasmania, Australia. ✉e-mail: yenh@ysfri.ac.cn

Supplementary Information

Decreased motility of flagellated microalgae grown in CO_2-induced acidified waters for over five years

Yitao Wang[1,2], Xiao Fan[1], Guang Gao[3], John Beardall[3,4], Kazuo Inaba[5], Jason M. Hall-Spencer[5,6], Dong Xu[1], Xiaowen Zhang[1], Wentao Han[1], Andrew McMinn[7] and Naihao Ye[1,2*]

[1]Yellow Sea Fisheries Research Institute, Chinese Academy of Fishery Sciences, Qingdao, China
[2]Function Laboratory for Marine Fisheries Science and Food Production Processes, Qingdao National Laboratory for Marine Science and Technology, Qingdao, China
[3]State Key Laboratory of Marine Environmental Science & College of Ocean and Earth Sciences, Xiamen University, Xiamen 361005, China
[4]School of Biological Sciences, Monash University, Clayton, Victoria 3800, Australia
[5]Shimoda Marine Research Center, University of Tsukuba, Shizuoka, Japan
[6]School of Biological and Marine Sciences, University of Plymouth, PL4 8AA, UK.
[7]Institute of Antarctic and Southern Ocean Studies, University of Tasmania, P.O. Box 252-77, Tasmania 7001, Australia
*E-mail: yenh@ysfri.ac.cn

Supplementary Methods

Blue light induced *Microglena* sp. movement. Blue light density distribution with variations in incident irradiance was measured during the positive/negative phototaxis assays of *Microglena* sp., (Supplementary Fig. 8e). The average and instantaneous velocities of *Microglena* sp. under blue light were measured by referring to the method in main text.

Vertical cell spatial distribution. To visualize the cell distribution at the end of the light induction experiment, we calculated the cell numbers under each CO_2 gradient at different sampling sites after the vertical cell motion experiment (the section of **Vertical cell motion in the main text).** Algal cells cultured under different CO_2 levels were placed at one end of separate channels. The size and structure of these channels were exactly same and they were placed side by side. After the same light intensity induction, algal cells are redistributed in the channels. We considered cells numbers in the no. 1 sampling point for all (280-1, 400-1, 700-1, 1000-1, 1500-1, 2000-1) CO_2 gradients as a whole (100%), calculated the percentage of cells number for each CO_2 concentration, and marked the actual cell number (mean) on it (the bar). Sampling points no.2-10 were calculated in the same way. This data presentation shows the distribution of cells in the channels at the end of the experiment.

Horizontal cell spatial distribution. To visualize the cell distribution at the end of the light induction experiment, we calculated the cell numbers under each CO_2 gradient at different sampling sites after the horizontal cell motion experiment (the section of **Horizontal cell motion in the main text).** Algal cells cultured under different CO_2 levels were placed at one end of separate channels. The size and structure of these channels were exactly same and they were placed side by side. After the same light intensity induction, algal cells are redistributed in the channels. We considered cells numbers in the no. 1 sampling point for all (280-1, 400-1, 700-1, 1000-1, 1500-1, 2000-1) CO_2 gradients as a whole (100%), calculated the percentage of cells number for each CO_2 concentration, and marked the actual cell number (mean) on it (the bar). Sampling points no.2-10 were calculated in the same way. This data presentation shows the distribution of cells in the channels at the end of the experiment.

Distribution of *Microglena* sp. via spontaneous fluorescence. The procedure was based on Ueki et al (2016) method with improvements[30]. The distribution of cells reflects the velocity of cells with biomass estimated by chlorophyll fluorescence. Cells were washed in experimental solutions of different pH and kept under red light for more than 50 min before the assays. For the positive and negative phototaxis assays, 2 mL cell suspensions (~10^7 cells/mL) were placed into Petri dishes (35 mm in diameter, 10 mm thick), illuminated with a LED (positive phototaxis assays White, ~2 μmol photons$\cdot m^{-2}\cdot s^{-1}$; negative phototaxis assays White, ~200 μmol photons$\cdot m^{-2}\cdot s^{-1}$) from one side for 20 min, and photos taken with an Imaging-PAM (Walz, Effeltrich, Germany).

CO_2/pH manipulation. To distinguish the effects of carbonation vs. acidification, seawater medium was prepared using synthetic ocean water (SOW) to obtain the targeted CO_2 and pH levels, i.e., carbonated (CO_2 400 ppm + pH 8.1, CO_2 1000 ppm + pH 8.1 and CO_2 2000 ppm + pH 8.1), acidified (CO_2 400 ppm + pH 8.1, CO_2 400 ppm + pH 7.8 and CO_2 400 ppm + pH 7.5) conditions using benchtop fermentor (Minifors Bacteria, INFORS, Swiss). The carbonate chemistry of the *Microglena* sp. and *D. salina* medium was manipulated by adding different amounts of $NaHCO_3$ to the medium while maintaining a constant medium pH with 2 mM 4-(2- Hydroxyethyl)-1-piperazinepropanesulfonic acid (EPPS, Sigma Ultra), to achieve independent variation of CO_2 and pH[34]. The carbonate chemistry of the *C. reinhardtii* medium was manipulated by adding different

amounts of $NaHCO_3$ to the medium while maintaining a constant medium pH with 2 mM 2- [4-(2-hydroxyethyl) piperazin-1-yl] ethane sulfonic acid (HEPES, Sigma Ultra), to achieve independent variation of CO_2 and pH (Supplementary Tables 18-20). The cultures were grown semi-continuously and were pre-acclimated to experimental conditions for 30 days. The experimental methods refer to Vertical cell motion and Horizontal cell motion of are the same as the main text.

Detection of cytosolic Ca^{2+} concentrations. The Ca^{2+} level was indicated by a Ca^{2+}-sensitive fluorescent dye, Fluo-3/AM (Molecular Probe). The method was based on Chen et al (2014) method with improvements[35]. The log phase cells were cultured for 20 minutes under light intensity for positive and negative phototaxis, respectively. Then the algal pellet was obtained by centrifugation at the corresponding culture temperature at 4000 *g* for 3 minutes. The algal pellets were loaded with the fluorescent dyes of 5 mmol/L final concentration of acetoxymethyl ester form (AM) of fluo-3 and 50 mmol/L final concentration of sorbitol in the dark for 1 h. Loaded cells was subsequently rinsed 3 times in fresh iso-osmotic medium, and then harvested by centrifugation. Fluorescence images and mean fluorescence of cells were measured after 20 min of positive and negative phototaxis induction. The fluorescence settings were as follows: excitation = 488 nm, emission = 510–530 nm. Imaging of the cells were obtained with laser scanning confocal microscope (TCS SP5 II, LEICA, Germany).

Genetic adaptation to long term acidification. To query the potential genetic adaptation in genome, we performed the whole genome resequencing on the samples under 5 years CO_2 acidification in 400 ppm, 1000 ppm and 2000 ppm, and the algal samples of 5 years ago were also be sequenced as negative control. For each of the samples, three biological replicates were assayed independently. Genomic DNA was extracted using the Plant Genomic DNA kit (Tiangen, Beijing, China), and RNA was removed by incubating the DNA solution at 37°C with a DNase-free RNase A (Tiangen) for 30 min. DNA integrity was assessed using agarose gels and a NanoPhotometer® spectrophotometer (IMPLEN, Westlake Village, CA, USA). DNA was quantified with a Qubit® 2.0 Flurometer (Life Technologies, Carlsbad, CA, USA) using the Qubit® DNA Assay Kit. High quality DNA was used to perform whole-genome sequencing (WGS) employing an Illumina Hiseq 2500 platform. We used FastQC (Babraham Institute, http://www.bioinformatics.babraham.ac.uk/projects/fastqc/) to examine the overall sequencing quality of the raw reads. The FASTQ data were cleaned and trimmed using Trimmomatic[36] (SLIDINGWINDOW: 4:15, LEADING: 3, TRAILING: 3, ILLUMINACLIP: adapter. fa: 2: 30: 10). All short reads (< 36 bps) and broken pairs were discarded. The resulting high-quality reads were aligned to the corresponding genomes assemblies using SAMTOOLS[37], and Single nucleotide polymorphisms (SNPs) were called using bam-readcount (https://github.com/genome/bam-readcount). SNP counts per 100k bp length bin of each chromosome were calculated using in-house python script. To construct back-translated nucleotide alignments, protein alignments between HGTs and the corresponding MMSHs were generated using MUSCLE version 3.8.31 under the default settings[38], and thereafter, protein-coding DNA alignments were guided by their protein alignments and limited to un-gapped regions using ParaAT (Parallel Alignment and back-Translation tool)[39]. The Ka, Ks, ω (Ka/Ks) between HGTs and the corresponding MMSHs were calculated using KaKs Calculator 2.0 (http://evolution.genomics.org.cn/software.htm) under the model-selected (MS) setting.

Light distribution. Under laboratory conditions, a LED lamp was used as the light source, and the distribution of light in the experimental channel was measured by an underwater light meter (LI-

192, LI-COR, USA). In a uniform culture (~4 × 10^5 cells/mL), light is attenuated rapidly due to absorption by the algal cells. The light distribution in seawater was different to that in the cultures during the positive and negative phototaxis assays.

Growth curve. Culture growth rates were measured in 500 ml conical flasks containing 300 ml medium. The conical flasks were placed in the same phytotron chamber under a series of CO_2 concentrations (280, 400, 700, 1000, 1500, 2000 ppm). Cell density was measured every two days using a blood count plate. The generations were calculated as follows: $G = n \cdot d \cdot (\ln(N_{t2}/N_{t1})) / ((t_2 - t_1) \cdot \ln 2)$ (Equation 3)G: generations; n: year = 5; d: days= 365; N_{t1}: cell numbers of on day t_1; N_{t2}: cell numbers of on day t_2; t_1, t_2: sampling time; the factor ln2 reflects the that binary fission growth of cells.

Carbonate chemistry. Total alkalinity (TA) was measured using an 848 Titrino plus automatic titrator (Metrohm, Riverview, FL, USA) on 50 ml of GF/F filtered samples. pH was measured using a pH electrode (6010M, Jenco, USA). Temperature was measured using a mercury thermometer (YHZ-90271, Yuhuaze, China). Salinity was measured using a salinity meter (YK31SA, Luchang, China). Carbonate system parameters were calculated using the CO2SYS Package (Pierrot, Lewis, & Wallace, 2006) in Excel based on pH, temperature, salinity, and TA[40].

Supplementary Results and Discussion

Distribution of *Microglena* sp. via spontaneous fluorescence. In this experiment, the higher the fluorescence intensity, the higher the number of cells. The aggregation of cells is reflected by the color of fluorescence. The fluorescence intensity is shown in bar on the left of the picture, with red being the weakest and green the strongest (Supplementary Fig. 4). As shown in Supplementary Fig. 8, when the induced light intensity was 2 μmol photons·m^{-2}·s^{-1}, the cells showed positive phototaxis response, and the fluorescence intensity on the near side was higher than that on the far side. Comparing the algae treated with different CO_2, the 280 ppm treatment group showed the greatest difference in fluorescence intensity between the near-light side of the plate and the far-light side, with a black color on the far-light side indicating almost no cells. With the increase of carbon dioxide concentration, the fluorescence intensity on the far-light side began to increase, indicating that the movement distance of cells in a certain period of time decreased due to the decreased velocity. Similarly, in the negative phototaxis response, the difference fluorescence intensity on both sides of the plate decreased with decreased velocity.

Ca^{2+} concentrations effect on cell velocity. In terms of biological function of Ca^{2+}, it has been found that Ca^{2+} plays a major role in regulating the motion of cells[2,11,13,31]. Schmidt showed that low concentrations of Ca^{2+} (<10^{-6} M) induced forward swimming and high concentrations of Ca^{2+} (10^{-3} M) induced backwards swimming of *C. reinhardtii*[41]. Data presented here, with a Ca^{2+} concentration of 2*10^{-4} M (between 10^{-6} M and 10^{-3} M), *Microglena* sp. excreted Ca^{2+} under the positive phototaxis assay conditions and absorbed Ca^{2+} under the negative phototaxis assay treatment (Fig. 3g). In addition, elevated CO_2/acidification reduced the Ca^{2+} flux under positive and negative phototaxis assays. This suggests that *Microglena* sp. can regulate Ca^{2+} concentrations and that this plays a role in positive and negative phototaxis (Supplementary Fig. 20) and that acidification may reduce the Ca^{2+} flux resulting in a decrease in the velocity of cell motion (Fig. 1)[42,43]. Similar results were found in *C. reinhardtii* and *D. salina* assays (Extended data Fig. 1).

Growth curve. Although high CO_2 increases population growth in many chlorophytes and larger phytoplankton may better adapt to variable pH conditions [8, 44], the individual velocity of *Microglena* sp. becomes slower, increasing predation and survival risks. In addition, the lengthened DVM at higher CO_2 levels may become unfavorable (Fig. 4b).

Supplementary References

34. Shi, D., Hong, H., Su, X., Liao, L., Chang, S., & Lin, W. The physiological response of marine diatoms to ocean acidification: differential roles of seawater pCO_2 and pH. *J. Phycol.* **55**, 521-533 (2019).
35. Chen, H., Zhang, Y., He, C., & Wang, Q. Ca^{2+} signal transduction related to neutral lipid synthesis in an oil-producing green alga *Chlorella* sp. C2. Plant and Cell Physiology, **55**, 634-644 (2014).
36. Bolger, M., Lohse, M. & Usadel, B. Trimmomatic: a flexible trimmer for Illumina sequence data. *Bioinformatics* **30**, 2114-2120 (2014).
37. Li, H., Handsaker, B., Wysoker, A., Fennell, T., Ruan, J., Homer, N., ... & Durbin, R., The Sequence Alignment/Map format and SAMtools. *Bioinformatics* **25**, 2078-2079 (2009).

38. Edgar, R.C. MUSCLE: multiple sequence alignment with high accuracy and high throughput. *Nucleic Acids Res* **32**, 1792-1797 (2004).
39. Zhang, Z., Li, J., Zhao, X., Wang, J., Wong, G.K., Yu, J. KaKs_Calculator: Calculating Ka and Ks Through Model Selection and Model Averaging. *Genomics, Proteomics & Bioinformatics* **4**, 259-263 (2006).
40. Pierrot, D., Lewis, E., & Wallace, D. W. R. CO2SYS DOS Program developed for CO_2 system calculations. ORNL/CDIAC-105. Carbon Dioxide Information Analysis Center, Oak Ridge National Laboratory, US Department of Energy, Oak Ridge, TN. (2006).
41. Schmidt, J.A. & Eckert, R. Calcium couples flagellar reversal to photostimulation in *Chlamydomonas reinhardtii. Nature* **262**, 713-715 (1976).
42. Wheeler, G.L. & Brownlee, C. Ca^{2+} signaling in plants and green algae – changing channels. *Trends Plant Sci.* **13**, 506-514 (2008).
43. Inaba, K. Calcium sensors of ciliary outer arm dynein: functions and phylogenetic considerations for eukaryotic evolution. *Cilia* **4**, 6 (2015).
44. Brennan, G. & Collins, S. Growth responses of a green alga to multiple environmental drivers. *Nat. Clim. Change* **5**, 892 (2015).

Supplementary Figures

Supplementary Figure 1: Spatial distribution of *Microglena* sp. in the channel after adding sample at one end.

Supplementary Figure 2: Spatial distribution of *C. reinhardtii* and *D. salina* in the channel after adding the sample at one end.

Supplementary Figure 3: Spatial distribution of *Microglena* sp. induced by sunlight in the channel after adding the sample at one end.

Supplementary Figure 4: Positive and negative phototaxis were shown by chlorophyll fluorescence of *Microglena* sp..

Supplementary Figure 5: Average velocity of *Microglena* sp. under pH and CO_2.

Supplementary Figure 6: Average velocity of *C. reinhardtii* under pH and CO_2.

Supplementary Figure 7: Average velocity of *D. salina* under pH and CO_2.

Supplementary Figure 8: Channels for experiment and intensity distribution with variation of incident irradiance in channel at laboratory micro-small scale.

Supplementary Figure 9: Channels for experiment and intensity distribution with variation of incident irradiance in channel on the sea at field meso-scale.

Supplementary Figure 10: Diagram of laboratory micro-small scale and field mesoscale for cell motion and spatial distribution assay.

Supplementary Figure 11: Average velocity of *Microglena* sp. induced by blue light.

Supplementary Figure 12: Instantaneous velocity of *Microglena* sp. under blue light.

Supplementary Figure 13: Effect of CO_2 concentration on growth of *Microglena* sp..

Supplementary Figure 14: Effect of CO_2 concentration on growth of *C. reinhardtii* and *D. salina.*

Supplementary Figure 15: Difference of gene expression pattern between 400 and 1000ppm CO_2 treatment.

Supplementary Figure 16: Ca^{2+} concentration in *Microglena* sp. under CO_2 (280, 400, 700, 1000, 1500, 2000 ppm).

Supplementary Figure 17: Ca^{2+} concentration in *C. reinhardtii* and *D. salina* under CO_2 (400, 1000, 2000 ppm). Mean value represents the fluorescence intensity of the cells. Bar, 10μm.

Supplementary Figure 18: Comparison between overall SNPs count of *Microglena* sp. grown under normal (control, samples five years ago, marked in grey), 400ppm (red), 1000ppm (green) and 2000ppm (blue) CO_2 conditions.

Supplementary Figure 19: Profile of genetic mutations across reference genomes of *Microglena* sp. grown under normal (control, samples five years ago, marked in grey), 400ppm (blue), 1000ppm (yellow) and 2000 ppm (red) CO_2 conditions.

Supplementary Figure 20: The relative SNP level of genes of *Microglena* sp. related to algal motility under acidification gradients.

Supplementary Figure 21: The ratio of synonymous and non-synonymous mutations of *Microglena* sp. under acidification gradients.

Supplementary Tables

Supplementary Table 1. Repeated analysis of variance for the effects of positive and negative phototaxis on average velocity in *Microglena* sp. grown under various pCO_2 in the laboratory microscale experiment.

Supplementary Table 2. Repeated analysis of variance for the effects of positive and negative phototaxis on average velocity in *Microglena* sp. grown under various pCO_2 in the field mesoscale experiment.

Repeated analysis of variance for the effects of positive and negative phototaxis on average velocity in *C. reinhardtii* grown under various pCO_2 in the laboratory microscale experiment.

Supplementary Table 4. Repeated analysis of variance for the effects of positive and negative phototaxis on average velocity in *D. salina* grown under various pCO_2 in the laboratory microscale experiment.

Supplementary Table 5. Repeated analysis of variance for the effects of laboratory microscale and field mesoscale on average velocity in *Microglena* sp. grown under various pCO_2.

Supplementary Table 6. Repeated analysis of variance for the effects of positive and negative phototaxis on instantaneous velocity in *Microglena* sp., grown under various pCO_2, in the laboratory microscale experiment.

Supplementary Table 7. Repeated analysis of variance for the effects of positive and negative phototaxis on instantaneous velocity in *C. reinhardtii* grown under various pCO_2, in the laboratory microscale experiment.

Supplementary Table 8. Repeated analysis of variance for the effects of positive and negative phototaxis on instantaneous velocity in *D. salina* grown under various pCO_2 in the laboratory microscale experiment.

Supplementary Table 9. Repeated analysis of variance for the effects of white and blue light on average velocity in *Microglena* sp., grown under various pCO_2, in the vertical direction in the laboratory microscale experiment.

Supplementary Table 10. Repeated analysis of variance for the effects of white and blue light on average velocity in *Microglena* sp., grown under various pCO_2, in the horizontal direction in the laboratory microscale experiment.

Supplementary Table 11. Repeated analysis of variance for the effects of white and blue light on instantaneous velocity in *Microglena* sp., grown under various pCO_2, in the vertical direction in the laboratory microscale experiment.

Supplementary Table 12. Repeated analysis of variance for the effects of white and blue light on instantaneous velocity in *Microglena* sp., grown under various pCO_2, in the horizontal direction in the laboratory microscale experiment.

Supplementary Table 13. Annotations of flagella bending genes for RT-PCR.

Supplementary Table 14. Medium for *Microglena* sp..

Supplementary Table 15. Medium for *C. reinhardtii.*

Supplementary Table 16. Medium for *D. salina.*

Supplementary Table 17. Original carbonate system data (mean ± standard errors) determined from total alkalinity (TA) and pH at 6 °C, 32‰ salinity in the laboratory experiment using the CO2SYS Package.

Supplementary Table 18. Original carbonate system data (mean ± standard errors) determined from total alkalinity (TA) and pH at 6 °C, 32‰ salinity in the laboratory experiment using the CO2SYS Package in CO_2/pH manipulation experiment.

Supplementary Table 19. *C. reinhardtii* and *D. salina* culture conditions in natural seawater.

Supplementary Table 20. *C. reinhardtii* and *D. salina* culture conditions in artificial seawater.

Supplementary Table 21. Photosynthesis vs light curve.

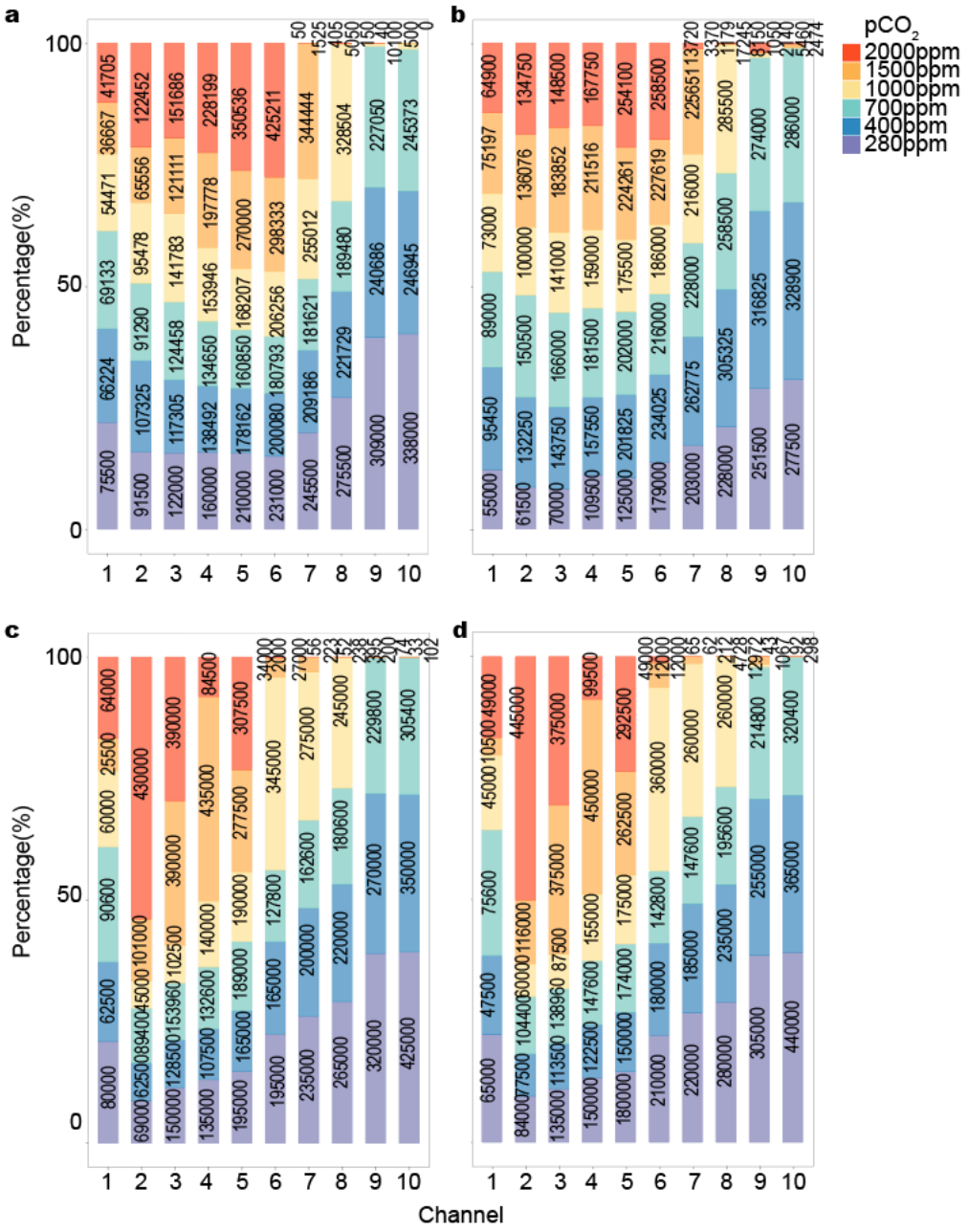

Supplementary Figure 1 | Spatial distribution of *Microglena* sp. in the channel after adding sample at one end. **a**, Positive phototaxis induced by white light in the vertical direction. **b**, Negative phototaxis induced by white light in the vertical direction. **c**, Positive phototaxis induced by white light in the horizontal direction. **d**, Negative phototaxis induced by white light in the horizontal direction. The ordinate (percentage) represents the proportion of cell number under different CO_2 concentration (280, 400, 700, 1000, 1500, 2000 ppm) to sum of all cells at the same sampling point. Bars of different colours represent different CO_2 concentrations. Numbers in the bars represent the actual number of cells at each sampling point. Mean values per experimental assay are given (n = 3).

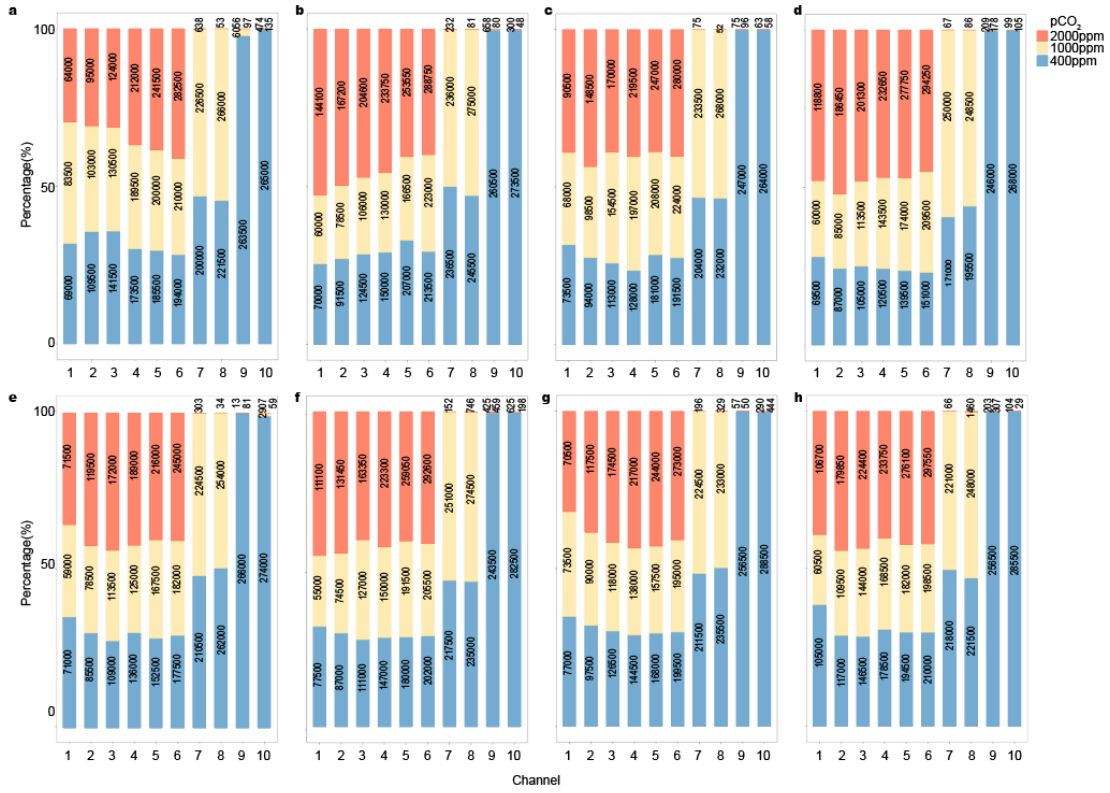

Supplementary Figure 2 | Spatial distribution of *C. reinhardtii* and *Dunaliella salina* in the channel after adding the sample at one end. **a**, *C. reinhardtii* positive phototaxis induced by white light in the vertical direction. **b**, *C. reinhardtii* negative phototaxis induced by white light in the vertical direction. **c**, *D. salina* positive phototaxis induced by white light in the vertical direction. **d**, *D. salina* negative phototaxis induced by white light in the vertical direction. **e**, *C. reinhardtii* positive phototaxis induced by white light in the horizontal direction. **f**, *C. reinhardtii* negative phototaxis induced by white light in the horizontal direction. **g**, *D. salina* positive phototaxis induced by white light in the horizontal direction. **h**, *D. salina* negative phototaxis induced by white light in the horizontal direction. The ordinate (percentage) represents the proportion of cell number under different CO_2 concentration (280, 400, 700, 1000, 1500, 2000 ppm) to sum of all cells at the same sampling point. Bars of different colours represent different CO_2 concentrations. Numbers in the bars represent the actual number of cells at each sampling point. Mean values per experimental assay are given (n = 3).

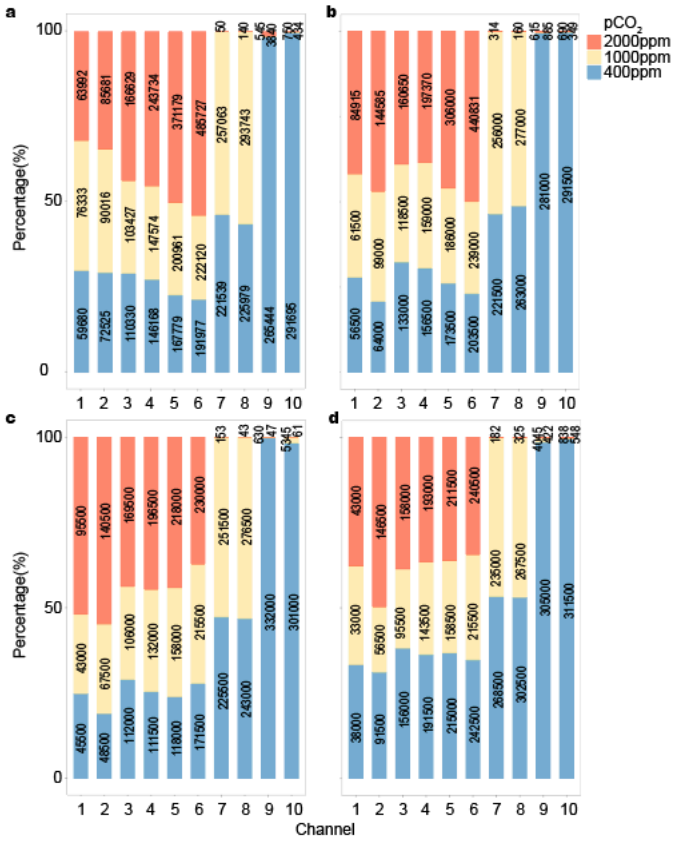

Supplementary Figure 3 | Spatial distribution of *Microglena* sp. induced by sunlight in the channel after adding the sample at one end. **a**, Positive phototaxis in the vertical direction. **b**, Negative phototaxis in the vertical direction. **c**, Positive phototaxis in the horizontal direction. **d**, Negative phototaxis in the horizontal direction. The ordinate (percentage) represents the proportion of cell number under different CO_2 concentration (280, 400, 700, 1000, 1500, 2000 ppm) to sum of all cells at the same sampling point. Bars of different colours represent different CO_2 concentrations. Numbers in the bars represent the actual number of cells at each sampling point. Mean values per experimental assay are given (n = 3).

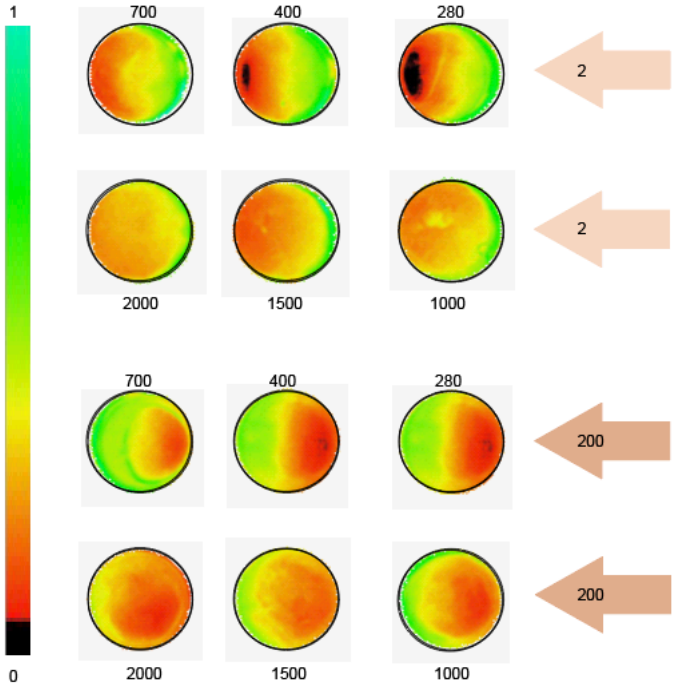

Supplementary Figure 4 | Positive and negative phototaxis was shown by chlorophyll fluorescence of *Microglena* sp.. Positive phototaxis induced by 2 µmol photons·m^{-2}·s^{-1} white light (light brown arrow). Negative phototaxis induced by 200 µmol photons·m^{-2}·s^{-1} white light (pale brown arrow). The fluorescence intensity reflects the number of cells. The scale of fluorescence as a proxy for cell number is shown on the left, the greener the colour, the more cells are present.

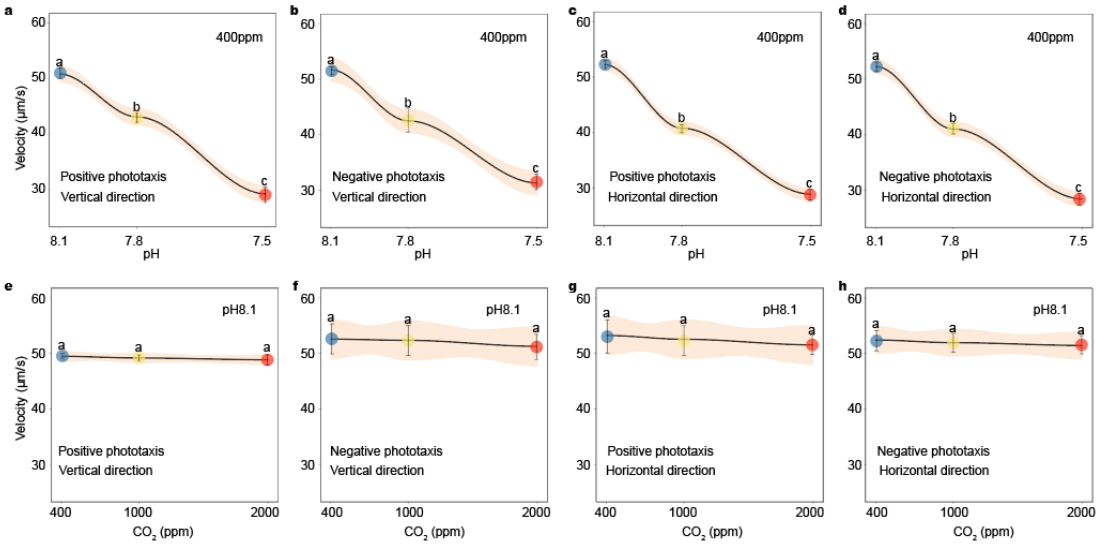

317

318 **Supplementary Figure 5 |.** Average velocity of *Microglena* sp. under pH and CO_2. **a**,
319 Positive phototaxis response in the vertical direction under different pH. **b**, Negative
320 phototaxis response in the vertical direction under different pH. **c**, Positive phototaxis
321 response in the horizontal direction under different pH. **d**, Negative phototaxis response
322 in the horizontal direction under different pH. **e**, Positive phototaxis response in the
323 vertical direction under different CO_2. **f**, Negative phototaxis response in the vertical
324 direction under different CO_2. **g**, Positive phototaxis response in the horizontal direction
325 under different CO_2. **h**, Negative phototaxis response in the horizontal direction under
326 different CO_2. Mean ± SD values per experimental assay are given (n = 3). Different
327 letters in superscript indicate significant differences ($p < 0.05$) among treatments.

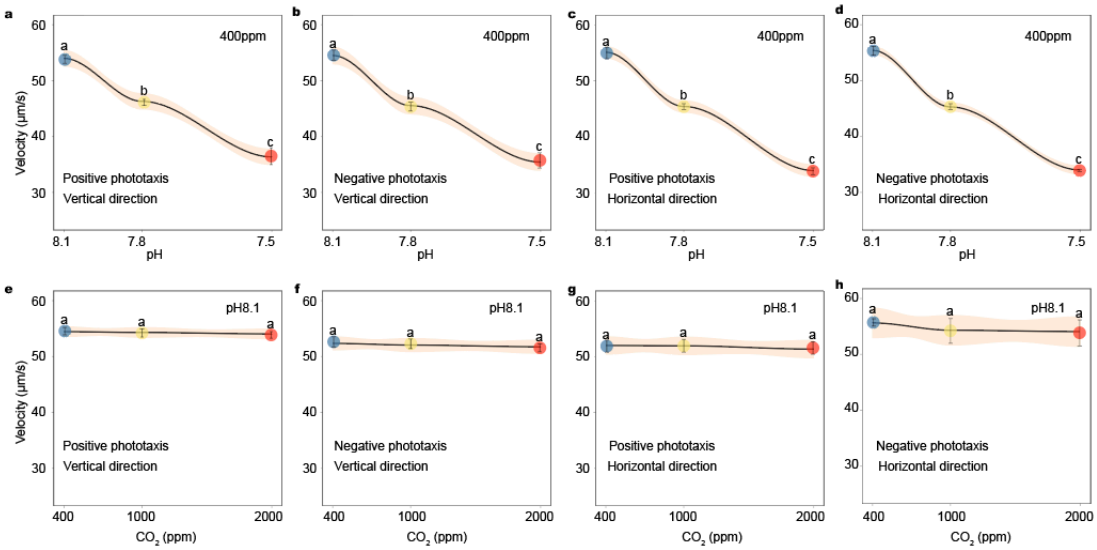

328

329 **Supplementary Figure 6 |.** Average velocity of *C. reinhardtii* under pH and CO_2. **a**,
330 Positive phototaxis response in the vertical direction under different pH. **b**, Negative
331 phototaxis response in the vertical direction under different pH. **c**, Positive phototaxis
332 response in the horizontal direction under different pH. **d**, Negative phototaxis response
333 in the horizontal direction under different pH. **e**, Positive phototaxis response in the
334 vertical direction under different CO_2. **f**, Negative phototaxis response in the vertical
335 direction under different CO_2. **g**, Positive phototaxis response in the horizontal direction
336 under different CO_2. **h**, Negative phototaxis response in the horizontal direction under
337 different CO_2. Mean ± SD values per experimental assay are given (n = 3). Different
338 letters in superscript indicate significant differences ($p < 0.05$) among treatments.

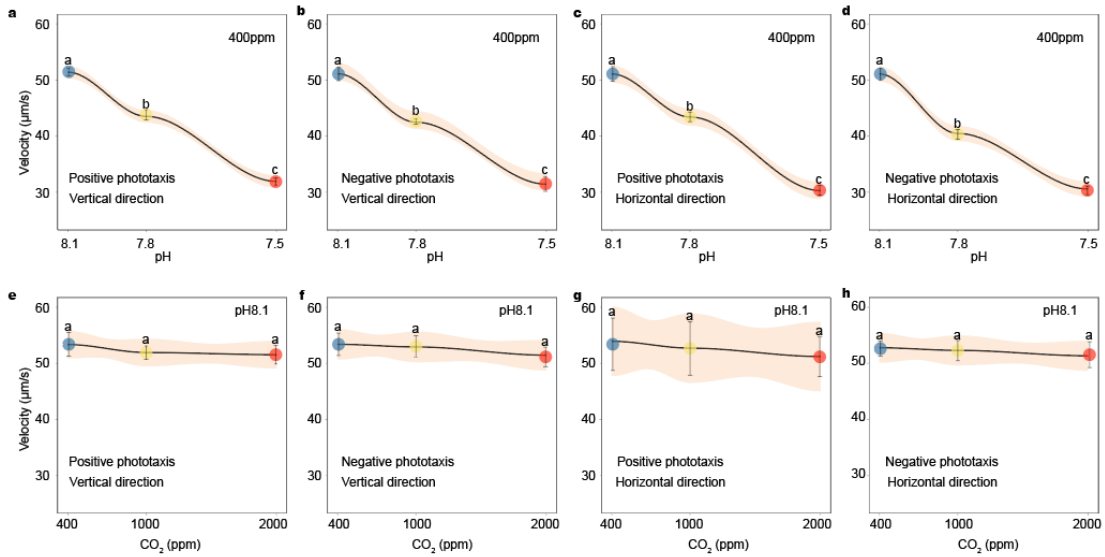

Supplementary Figure 7 |. Average velocity of *D. salina* under pH and CO_2 treatments. **a**, Positive phototaxis response in the vertical direction under different pH. **b**, Negative phototaxis response in the vertical direction under different pH. **c**, Positive phototaxis response in the horizontal direction under different pH. **d**, Negative phototaxis response in the horizontal direction under different pH. **e**, Positive phototaxis response in the vertical direction under different CO_2. **f**, Negative phototaxis response in the vertical direction under different CO_2. **g**, Positive phototaxis response in the horizontal direction under different CO_2. **h**, Negative phototaxis response in the horizontal direction under different CO_2. Mean ± SD values per experimental assay are given (n = 3). Different letters in superscript indicate significant differences ($p < 0.05$) among treatments.

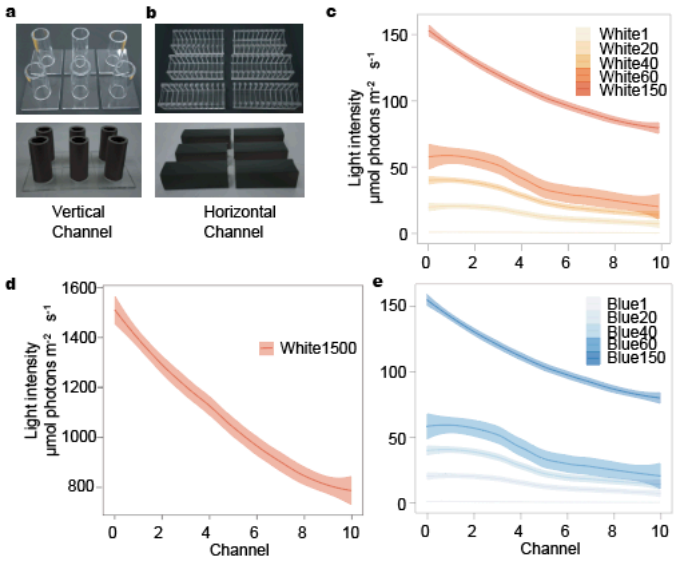

Supplementary Figure 8 | Channels for experiment and light intensity distribution with different incident irradiances in a channel at the laboratory micro- scale. **a**, Vertical experimental channels. For cell motion experiments, channel was cylindrical, with an inner diameter of 4.4 cm and a height of 11 cm. For cell spatial distribution experiments, channel was cylindrical, with an inner diameter of 4.4 cm and a height of 10 cm. **b**, Horizontal experimental channels. For cell motion experiments, channel was oblong with a section of a square with a diameter of 4 cm, and channels were evenly divided into 11 parts with a width of 1cm each. For cell spatial distribution experiments, channel was oblong with a section of a square with a diameter of 4cm, and channels were evenly divided into 10 parts with a width of 1cm each. **c**, Distribution of white light in pure seawater. The x axis represent position in the channel, the width of each position is 1cm (same in below figures). **d,** Distribution of white light as photophobic light of *C. reinhardtii* and *D. salina* in pure seawater. **e,** Distribution of blue light in pure seawater. Mean ± SD values per experimental assay are given (n = 3).

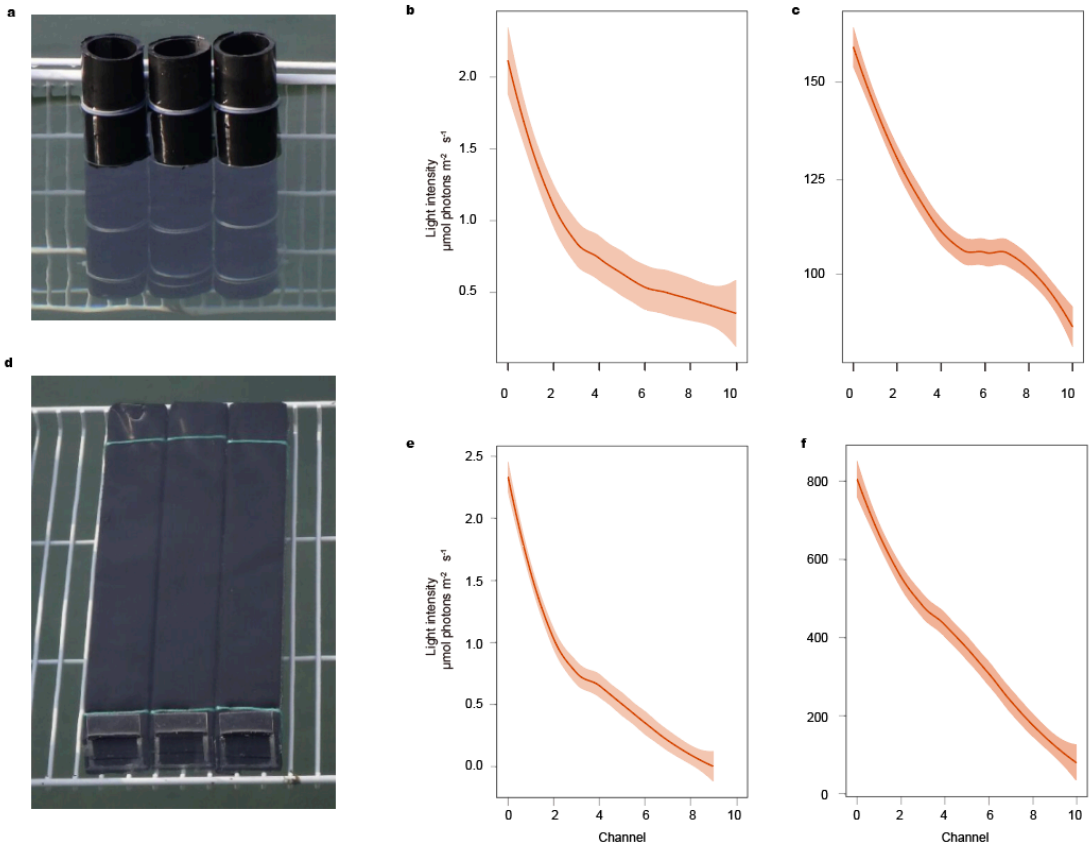

Supplementary Figure 9 | Channels for experiment and light intensity distribution with variation of incident irradiance in a channel at sea at the field meso-scale. **a**, Vertical experimental channels. **b**, Distribution of natural light in vertical channels under positive phototaxis. **c**, Distribution of natural light in vertical channels under negative phototaxis. **d**, Horizontal experimental channels. **e**, Distribution of natural light in horizontal channels under positive phototaxis. **f**, Distribution of natural light in horizontal channels under negative phototaxis. Mean ± SD values per experimental assay are given (n = 3).

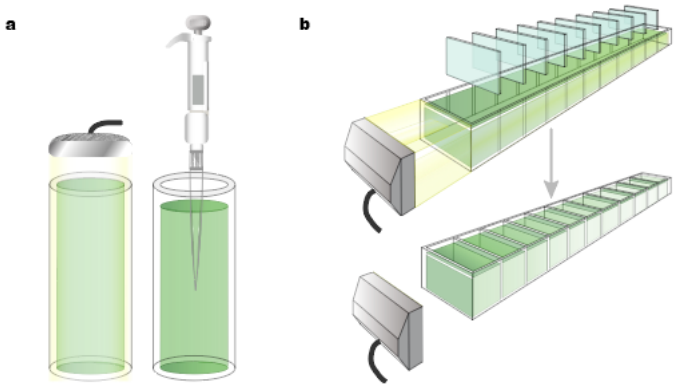

Supplementary Figure 10 | Diagram of laboratory micro-small scale and field mesoscale for cell motion and spatial distribution assay. **a**, Positive and negative phototaxis motion assay at the vertical in an 11cm channel. **b**, Positive and negative phototaxis motion assay at the horizontal in an 11cm channel, which is divided into 11 equal parts.

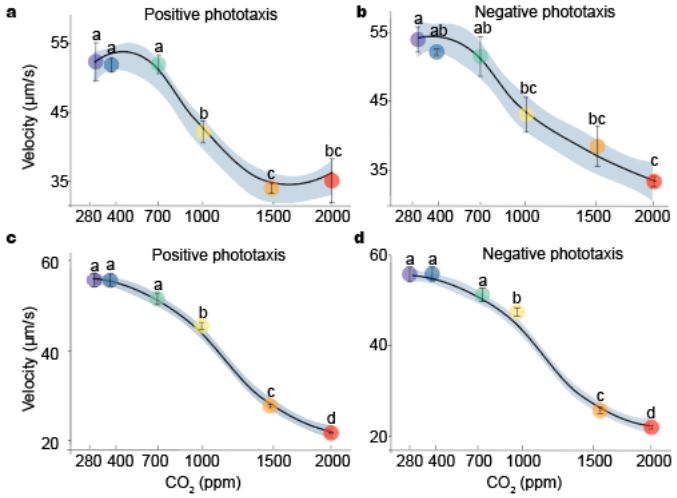

Supplementary Figure 11 | Average velocity of *Microglena* sp. induced by blue light. **a,** Positive phototaxis induced by blue light in the vertical direction. **b,** Negative phototaxis induced by blue light in the vertical direction. **c,** Positive phototaxis induced by blue light in the horizontal direction. **d,** Negative phototaxis induced by white light in the horizontal direction.

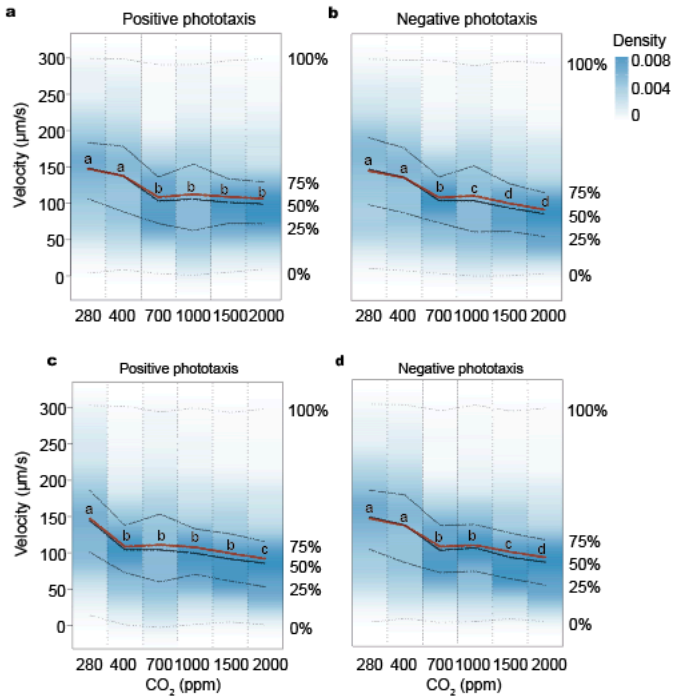

Supplementary Figure 12 | Instantaneous velocity of *Microglena* sp. under blue light. **a**, Positive phototaxis induced by blue light in the vertical direction. **b**, Negative phototaxis induced by blue light in the vertical direction. **c**, Positive phototaxis induced by blue light in the horizontal direction. **d**, Negative phototaxis induced by blue light in the horizontal direction. The colour scale indicates the density of the cell distribution under various velocities. A total of 300 data points was collected for each experimental treatment. The five dotted lines correspond to 0%, 25%, 50%, 75%, 100%, respectively. Each dotted line represents the cumulative ratio, the number of cells below the dotted line as a percentage of the total number of cells. The solid line represents the average velocity and letters indicate significant differences between CO_2 treatments ($p < 0.05$). Different letters in superscript indicate significant differences ($p < 0.05$) among treatments (Kruskal Wallis test followed by Dunn's post-hoc test).

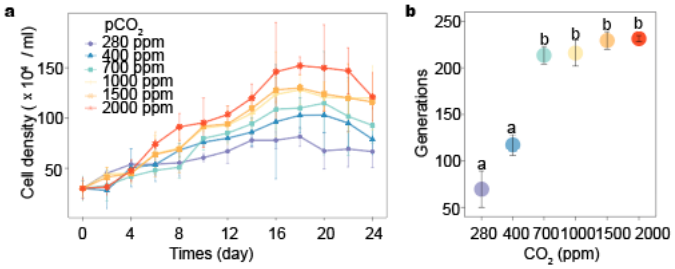

Supplementary Figure 13 | CO_2 concentration effects on growth of *Microglena* sp.. **a**, Growth curve. **b**, Generations in five years. Mean ± SD values per experimental assay are given (n = 3). Different letters in superscript indicate significant differences ($p < 0.05$) among treatments.

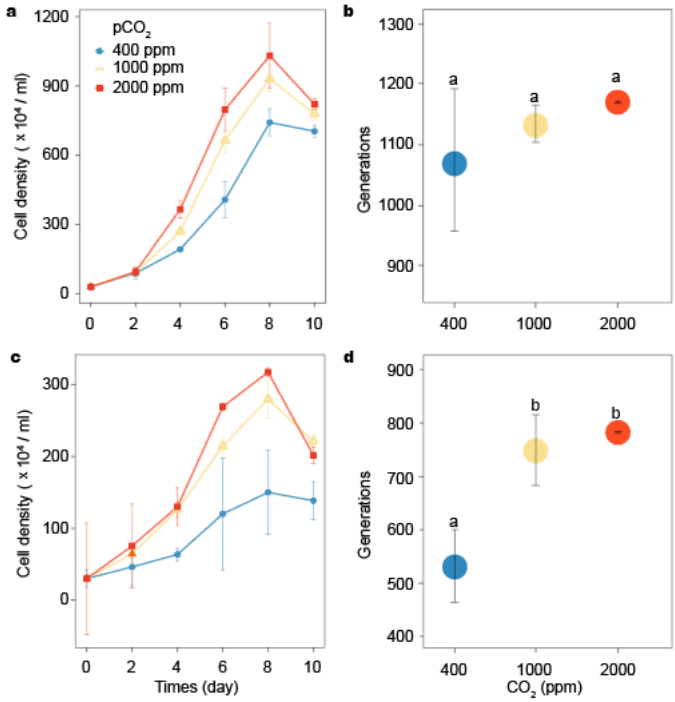

Supplementary Figure 14 | CO_2 concentration effects on growth of *C. reinhardtii* and *D. salina*. **a**, Growth curve of *C. reinhardtii*. **b**, Generations of *C. reinhardtii* in five years. **c,** Growth curve of *D. salina*. **d,** Generations of *D. salina.* Mean ± SD values per experimental assay are given (n = 3). Different letters in superscript indicate significant differences ($p < 0.05$) among treatments.

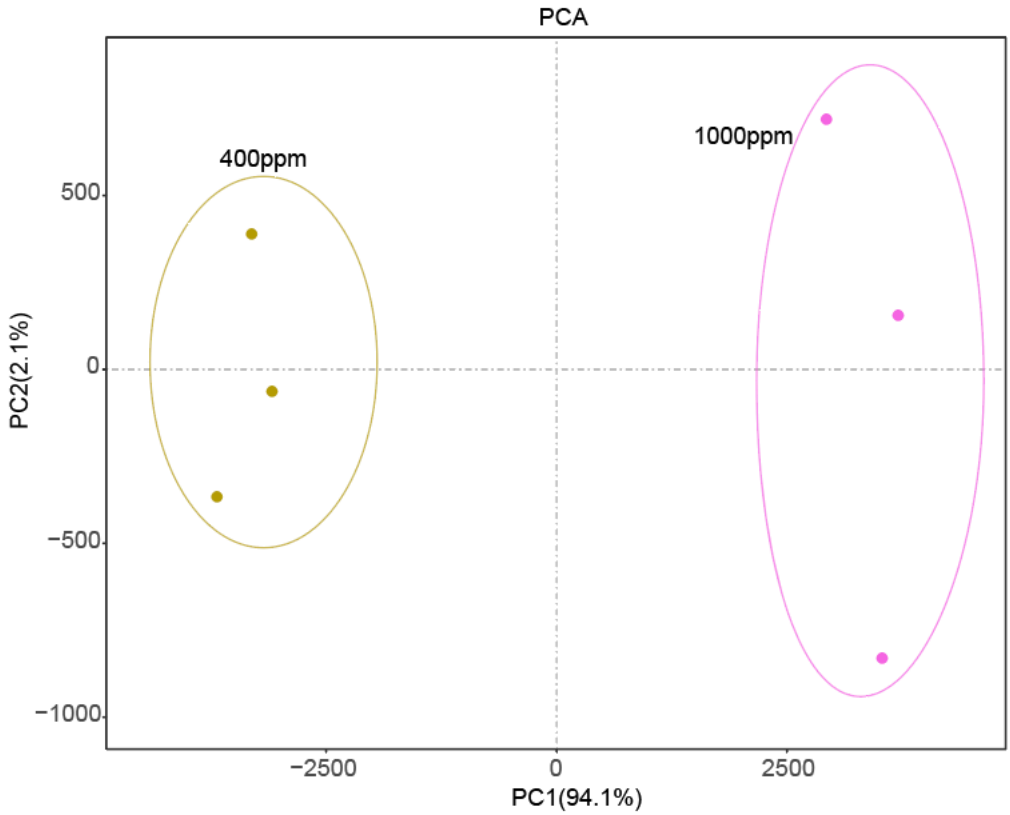

411

412 **Supplementary Figure 15** | Difference of gene expression pattern between 400 and
413 1000ppm CO_2 treatment.

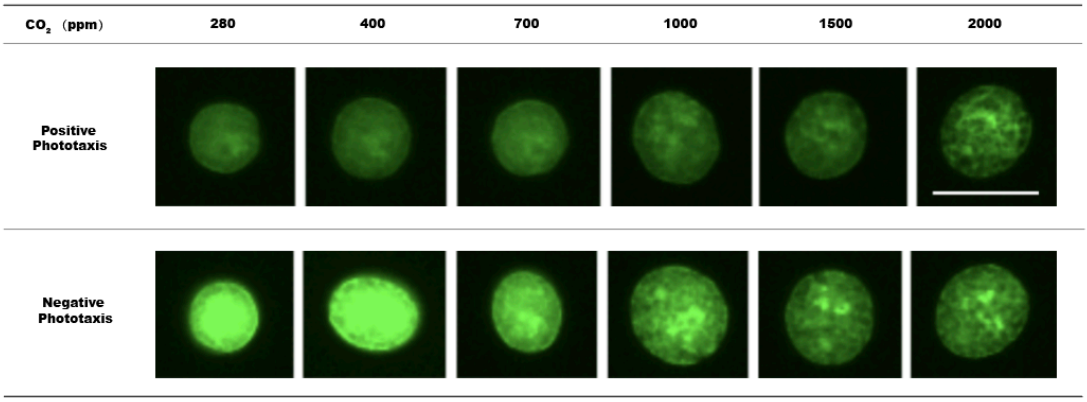

414

415 **Supplementary Figure 16 |** Ca^{2+} concentration in *Microglena* sp. under CO_2
416 concentration (280, 400, 700, 1000, 1500, 2000 ppm). The white bar represents the
417 length of 20 μm.
418

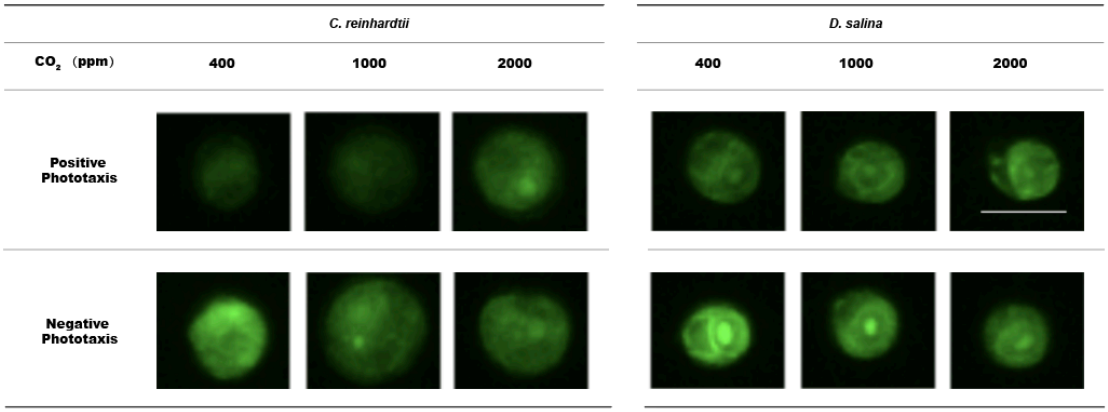

Supplementary Figure 17 | Ca^{2+} concentration in *C. reinhardtii* and *D. salina* under CO_2 concentration (400, 1000, 2000 ppm). Bar, 10μm.

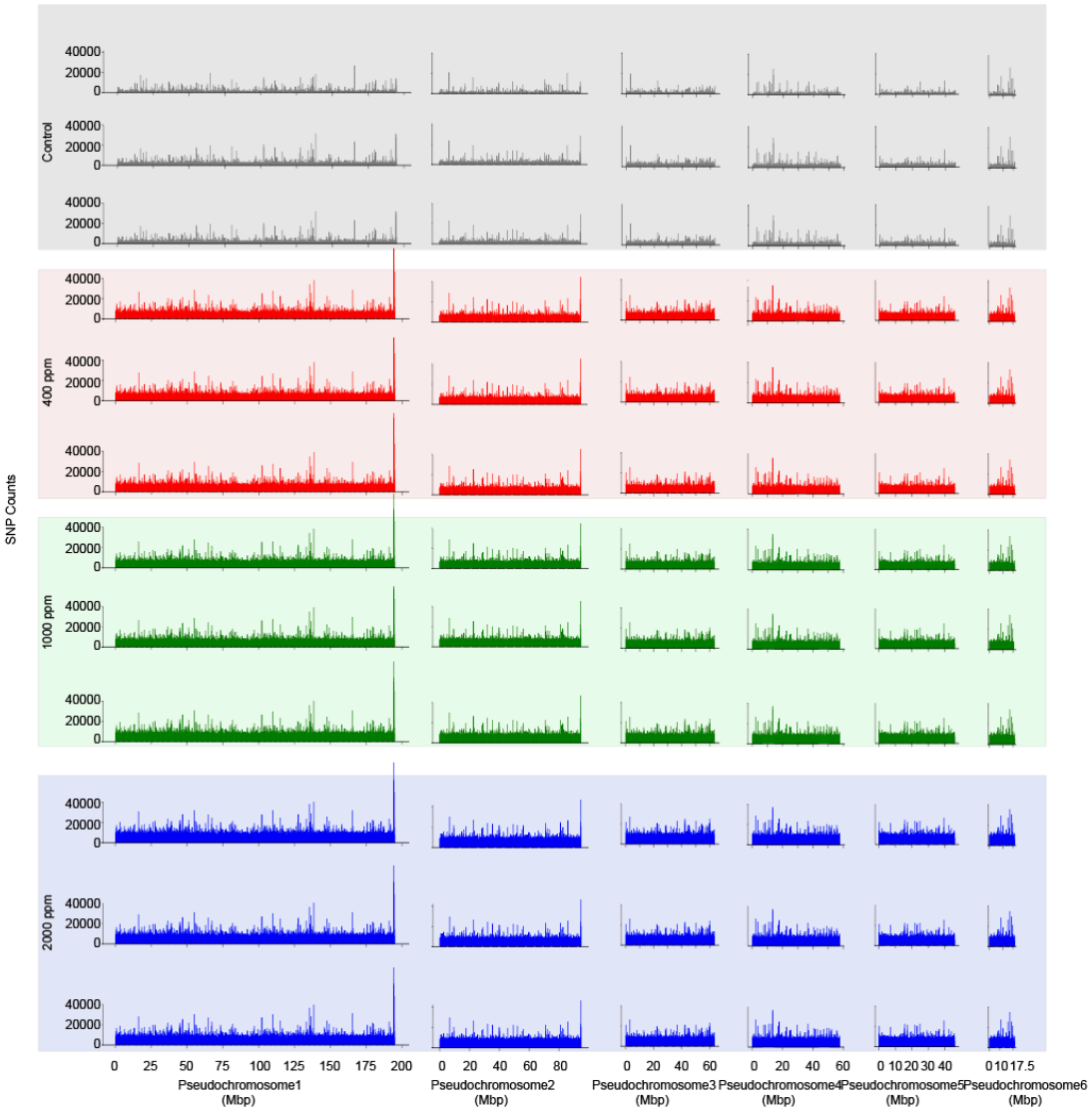

Supplementary Figure 18 | Comparison between overall SNPs count of *Microglena* sp.. grown under normal (control, samples five years ago, marked in grey), 400 ppm (red), 1000 ppm (green) and 2000 ppm (blue) CO_2 conditions.

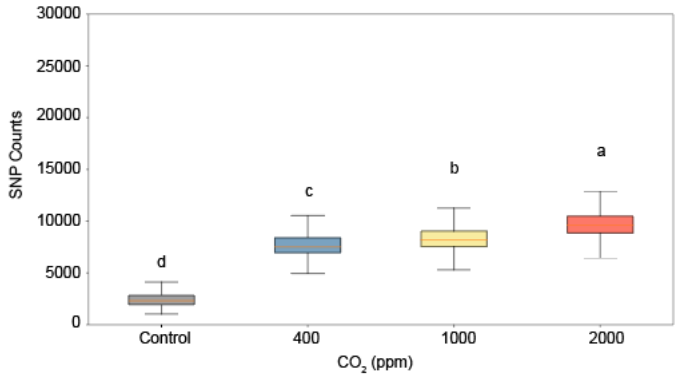

Supplementary Figure 19 | Profile of genetic mutations across reference genomes of *Microglena* sp.. grown under normal (control, samples five years ago, marked in grey), 400 ppm (blue), 1000 ppm (yellow) and 2000 ppm (red) CO_2 conditions. Different letters in superscript indicate significant differences ($p < 0.05$) among treatments.

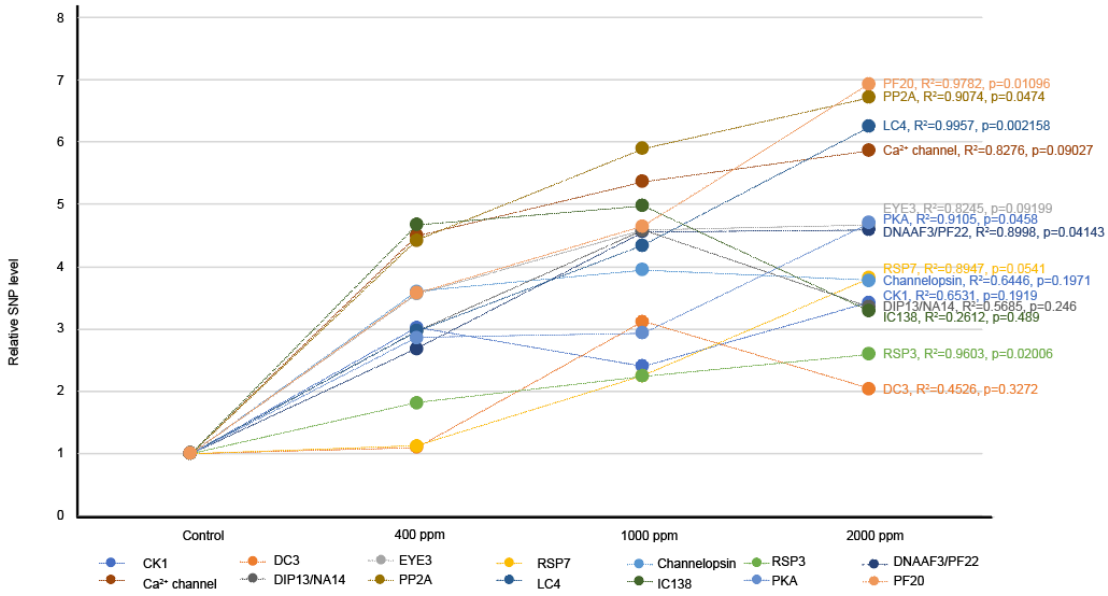

Supplementary Figure 20 | The relative SNP level of genes of *Microglena* sp.. related to algal motility under acidification gradients. SNP level=SNP counts/gene length. The SNP level under each acidification gradient is divided by that of the control, and is termed the relative SNP level.

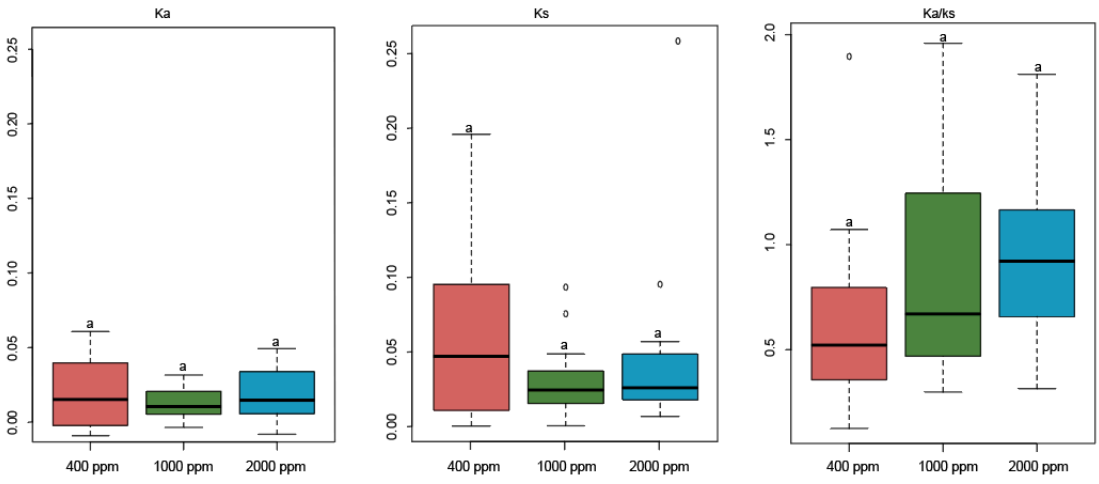

Supplementary Figure 21 | The ratio of synonymous and non-synonymous mutations of *Microglena* sp.. under acidification gradients.

Supplementary Table 1. Repeated analysis of variance for the effects of positive and negative phototaxis on average velocity in *Microglena* sp. grown under various pCO_2 used in the laboratory microscale experiment. R_V means ratio of velocity of positive phototaxis to velocity of negative phototaxis and Sig. means p value. Mean ± SD values per experimental assay are given (n = 3).

Motion direction	**CO_2 treatment (ppm)**	**Velocity**	
		R_V	**Sig.**
Vertical direction	**280**	<1	0.075
Vertical direction	**400**	<1	0.69
Vertical direction	**700**	>1	0.149
Vertical direction	**1000**	>1	0.471
Vertical direction	**1500**	>1	0.01
Vertical direction	**2000**	>1	0.02
Horizontal direction	**280**	<1	0.768
Horizontal direction	**400**	<1	0.709
Horizontal direction	**700**	<1	0.679
Horizontal direction	**1000**	<1	0.514
Horizontal direction	**1500**	<1	0.808
Horizontal direction	**2000**	<1	0.29

Supplementary Table 2. Repeated analysis of variance for the effects of positive and negative phototaxis on average velocity in *Microglena* sp. grown under various pCO_2 in the field mesoscale experiment. R_V means ratio of velocity of positive phototaxis to velocity of negative phototaxis and Sig. means p value. Mean ± SD values per experimental assay are given (n = 3).

Motion direction	**CO_2 treatment (ppm)**	**Velocity**	
		R_V	**Sig.**
Vertical direction	**400**	<1	0.834
Vertical direction	**1000**	>1	0.916
Vertical direction	**2000**	>1	0.401
Horizontal direction	**400**	>1	0.331
Horizontal direction	**1000**	<1	0.764
Horizontal direction	**2000**	<1	0.283

Supplementary Table 3. Repeated analysis of variance for the effects of positive and negative phototaxis on average velocity in *C. reinhardtii* grown under various pCO_2 in the laboratory microscale experiment. R_V means ratio of velocity of positive phototaxis to velocity of negative phototaxis and Sig. means p value. Mean ± SD values per experimental assay are given (n = 3).

Motion direction	**CO_2 treatment (ppm)**	**Velocity**	
		R_V	**Sig.**
Vertical direction	**400**	<1	0.247
Vertical direction	**1000**	<1	0.13
Vertical direction	**2000**	>1	0.087
Horizontal direction	**400**	>1	0.603
Horizontal direction	**1000**	<1	0.738
Horizontal direction	**2000**	<1	0.791

Supplementary Table 4. Repeated analysis of variance for the effects of positive and negative phototaxis on average velocity in *D. salina* grown under various pCO_2 in the laboratory microscale experiment. R_V means ratio of velocity of positive phototaxis to velocity of negative phototaxis and Sig. means p value. Mean ± SD values per experimental assay are given (n = 3).

Motion direction	**CO_2 treatment (ppm)**	**Velocity**	
		R_V	**Sig.**
Vertical direction	**400**	<1	0.74
Vertical direction	**1000**	<1	0.514
Vertical direction	**2000**	>1	0.6
Horizontal direction	**400**	>1	0.233
Horizontal direction	**1000**	>1	0.798
Horizontal direction	**2000**	>1	0.288

Supplementary Table 5. Repeated analysis of variance for the effects of laboratory microscale and field mesoscale on average velocity in *Microglena* sp. grown under various pCO_2. R_V means ratio of velocity of positive phototaxis to velocity of negative phototaxis and Sig. means p value. Mean ± SD values per experimental assay are given (n = 3).

Motion direction	Reaction to light	CO_2 treatment (ppm)	Velocity	
			R_V	Sig.
Vertical direction	**Phototaxis**	**400**	<1	0.214
Vertical direction	**Phototaxis**	**1000**	>1	0.91
Vertical direction	**Phototaxis**	**2000**	<1	0.611
Vertical direction	**Photophobism**	**400**	<1	0.393
Vertical direction	**Photophobism**	**1000**	<1	0.275
Vertical direction	**Photophobism**	**2000**	<1	0.182
Horizontal direction	**Phototaxis**	**400**	<1	0.627
Horizontal direction	**Phototaxis**	**1000**	>1	0.665
Horizontal direction	**Phototaxis**	**2000**	<1	0.001
Horizontal direction	**Photophobism**	**400**	>1	0.122
Horizontal direction	**Photophobism**	**1000**	>1	0.87
Horizontal direction	**Photophobism**	**2000**	<1	0.00

Supplementary Table 6. Repeated analysis of variance for the effects of positive and negative phototaxis on instantaneous velocity in *Microglena* sp. grown under various pCO_2 in the laboratory microscale experiment. R_V means ratio of velocity of positive phototaxis to velocity of negative phototaxis and Sig. means p value. Mean ± SD values per experimental assay are given (n = 3).

Motion direction	**CO_2 treatment (ppm)**	**Velocity**	
		R_V	**Sig.**
Vertical direction	**280**	>1	0.000
Vertical direction	**400**	>1	0.000
Vertical direction	**700**	>1	0.000
Vertical direction	**1000**	>1	0.000
Vertical direction	**1500**	>1	0.139
Vertical direction	**2000**	>1	0.000
Horizontal direction	**280**	>1	0.000
Horizontal direction	**400**	<1	0.000
Horizontal direction	**700**	>1	0.000
Horizontal direction	**1000**	>1	0.003
Horizontal direction	**1500**	>1	0.000
Horizontal direction	**2000**	>1	0.000

Supplementary Table 7. Repeated analysis of variance for the effects of positive and negative phototaxis on instantaneous velocity in *C. reinhardtii* grown under various pCO_2 in the laboratory microscale experiment. R_V means ratio of velocity of positive phototaxis to velocity of negative phototaxis and Sig. means p value. Mean ± SD values per experimental assay are given (n = 3).

Motion direction	**CO_2 treatment (ppm)**	**Velocity**	
		R_V	**Sig.**
Vertical direction	**400**	<1	0.000
Vertical direction	**1000**	<1	0.000
Vertical direction	**2000**	>1	0.003
Horizontal direction	**400**	>1	0.000
Horizontal direction	**1000**	>1	0.000
Horizontal direction	**2000**	>1	0.001

Supplementary Table 8. Repeated analysis of variance for the effects of positive and negative phototaxis on instantaneous velocity in *D. salina* grown under various pCO_2 in the laboratory microscale experiment. R_V means ratio of velocity of positive phototaxis to velocity of negative phototaxis and Sig. means p value. Mean ± SD values per experimental assay are given (n = 3).

Motion direction	**CO_2 treatment (ppm)**	**Velocity**	
		R_V	**Sig.**
Vertical direction	**400**	<1	0.004
Vertical direction	**1000**	<1	0.000
Vertical direction	**2000**	>1	0.140
Horizontal direction	**400**	>1	0.010
Horizontal direction	**1000**	>1	0.000
Horizontal direction	**2000**	>1	0.000

Supplementary Table 9. Repeated analysis of variance for the effects of white and blue light on average velocity in *Microglena* sp. grown under various pCO_2 in vertical direction in the laboratory microscale experiment. R_V means ratio of velocity of white light to velocity of blue light and Sig. means p value. Mean ± SD values per experimental assay are given (n = 3).

Motion direction	**CO_2 treatment (ppm)**	**Velocity**	
		R_V	**Sig.**
Positive phototaxis	**280**	>1	0.940
Positive phototaxis	**400**	<1	0.084
Positive phototaxis	**700**	<1	0.086
Positive phototaxis	**1000**	<1	0.801
Positive phototaxis	**1500**	>1	0.000
Positive phototaxis	**2000**	<1	0.786
Negative phototaxis	**280**	>1	0.419
Negative phototaxis	**400**	<1	0.788
Negative phototaxis	**700**	<1	0.359
Negative phototaxis	**1000**	<1	0.528
Negative phototaxis	**1500**	<1	0.186
Negative phototaxis	**2000**	<1	0.346

Supplementary Table 10. Repeated analysis of variance for the effects of white and blue light on average velocity in *Microglena* sp. grown under various pCO_2 in horizontal direction in the laboratory microscale experiment. R_V means ratio of velocity of white light to velocity of blue light and Sig. means p value. Mean ± SD values per experimental assay are given (n = 3).

Motion direction	**CO_2 treatment (ppm)**	**Velocity**	
		R_V	**Sig.**
Positive phototaxis	**280**	<1	0.708
Positive phototaxis	**400**	<1	0.693
Positive phototaxis	**700**	<1	0.664
Positive phototaxis	**1000**	>1	0.684
Positive phototaxis	**1500**	>1	0.530
Positive phototaxis	**2000**	<1	0.932
Negative phototaxis	**280**	>1	0.609
Negative phototaxis	**400**	<1	0.562
Negative phototaxis	**700**	<1	0.538
Negative phototaxis	**1000**	<1	0.756
Negative phototaxis	**1500**	>1	0.143
Negative phototaxis	**2000**	>1	0.905

Supplementary Table 11. Repeated analysis of variance for the effects of white and blue light on instantaneous velocity in *Microglena* sp. grown under various pCO_2 in vertical direction in the laboratory microscale experiment. R_V means ratio of velocity of white light to velocity of blue light and Sig. means p value. Mean ± SD values per experimental assay are given (n = 3).

Motion direction	**CO_2 treatment (ppm)**	**Velocity**	
		R_V	**Sig.**
Positive phototaxis	**280**	>1	0.000
Positive phototaxis	**400**	>1	0.000
Positive phototaxis	**700**	<1	0.000
Positive phototaxis	**1000**	<1	0.000
Positive phototaxis	**1500**	<1	0.000
Positive phototaxis	**2000**	<1	0.000
Negative phototaxis	**280**	>1	0.000
Negative phototaxis	**400**	>1	0.000
Negative phototaxis	**700**	<1	0.000
Negative phototaxis	**1000**	<1	0.000
Negative phototaxis	**1500**	<1	0.000
Negative phototaxis	**2000**	<1	0.000

Supplementary Table 12. Repeated analysis of variance for the effects of white and blue light on instantaneous velocity in *Microglena* sp. grown under various pCO_2 in horizontal direction in the laboratory microscale experiment. R_V means ratio of velocity of white light to velocity of blue light and Sig. means p value. Mean ± SD values per experimental assay are given (n = 3).

Motion direction	**CO_2 treatment (ppm)**	**Velocity**	
		R_V	**Sig.**
Positive phototaxis	**280**	>1	0.000
Positive phototaxis	**400**	>1	0.000
Positive phototaxis	**700**	>1	0.000
Positive phototaxis	**1000**	<1	0.000
Positive phototaxis	**1500**	<1	0.000
Positive phototaxis	**2000**	>1	0.000
Negative phototaxis	**280**	>1	0.000
Negative phototaxis	**400**	>1	0.000
Negative phototaxis	**700**	>1	0.000
Negative phototaxis	**1000**	>1	0.000
Negative phototaxis	**1500**	<1	0.009
Negative phototaxis	**2000**	<1	0.992

487 Supplementary Table 13. Annotations of flagella bending genes for RT-PCR.

Gene ID	Predicted function	Nr Annotation
MigICE16000	Voltage gated calcium channel CAV7	XP_001690493.1 voltage-gated Ca^{2+} channel, alpha subunit [*Chlamydomonas reinhardtii*]
MigICE11569	RSP7	AOM63275.1 calmodulin [*Chlamydomonas* sp. ICE-L]
MigICE12547	Channelopsin1	AER58219.1 channelopsin 1 [*Haematococcus lacustris*]
MigICE10361	Eyespot assembly protein EYE3	XP_001699977.1 eyespot assembly protein, ABC1 kinase family [*Chlamydomonas reinhardtii*]
MigICE08486	CK1	XP_001693999.1 ser/thr kinase [*Chlamydomonas reinhardtii*]
MigICE16283	PP2A	XP_001700181.1 PP2A-twin subunit [*Chlamydomonas reinhardtii*]
MigICE04581	PKA	XP_001693385.1 predicted protein, partial [*Chlamydomonas reinhardtii*]
MigICE14893	RSP3	KXZ49444.1 RSP3 protein [*Gonium pectorale*]
MigICE05195	PF20	AAB41727.1 PF20 [*Chlamydomonas reinhardtii*]
MigICE09498	DC3	GAQ81162.1 calmodulin [*Klebsormidium nitens*]
MigICE16837	LC4	XP_001690249.1 flagellar outer dynein arm 18 kDa light chain LC4 [*Chlamydomonas reinhardtii*]
MigICE04131	IC138	XP_001696921.1 flagellar inner dynein arm I1 intermediate chain IC138 [*Chlamydomonas reinhardtii*]
MigICE16200	Flagella Deflagellation inducible protein DIP13/NA14	XP_001697145.1 deflagellation inducible protein [*Chlamydomonas reinhardtii*]
MigICE14891	Dynein assembly protein DNAAF3/PF22	AEC04845.1 axonemal dynein assembly protein PF22 [*Chlamydomonas reinhardtii*]

488

489 Supplementary Table 14. Medium for *Microglena* sp..

Provasoli Stock Solution			
Component	**Element type**	**Initial concentration**	**End concentration**
II	$Fe(NH_4)_2(SO_4)_2•6H_2O$	2.738 mg L^{-1}	/
	Na_2EDTA	2.578 mg L^{-1}	/
III	Na_2EDTA	3.906 mg L^{-1}	/
	H_3BO_3	4.453 mg L^{-1}	/
	$FeCl_3•6H_2O$	0.191mg L^{-1}	/
	$MnCl_2•4H_2O$	0.57mg L^{-1}	/
	$ZnSO_4•7H_2O$	0.008 mg L^{-1}	/
	$CoCl_2•6H_2O$	0.0156 mg L^{-1}	/
N	NH_4NO_3	51.418 mg L^{-1}	15-25 mg L^{-1}
P	$NaH_2PO_4•2H_2O$	8.512 mg L^{-1}	0.01-0.02 mg L^{-1}

490

Supplementary Table 15. Medium for *C. reinhardtii*.

Provasoli Stock Solution			
Component	**Element type**	**Initial concentration**	**End concentration**
I	H_3BO_3	1 mg L^{-1}	/
	$ZnSO_4•7H_2O$	1 mg L^{-1}	/
	$MnSO_4•H_2O$	0.303 mg L^{-1}	/
	$CoCl_2•6H_2O$	0.2 mg L^{-1}	/
	$Na_2MoO_4•2H_2O$	0.2 mg L^{-1}	/
	$CuSO_4•5H_2O$	0.0625 mg L^{-1}	/
II	$Na_3C_6H_5O_7•2H_2O$	500 mg L^{-1}	/
III	$FeCl_3•6H_2O$	10 mg L^{-1}	/
IV	$CaCl_2•2H_2O$	53 mg L^{-1}	/
V	$MgSO_4•7H_2O$	300 mg L^{-1}	/
VI	NH_4NO_3	300 mg L^{-1}	1-5 mg L^{-1}
VII	KH_2PO_4	100 mg L^{-1}	0.01-0.02 mg L^{-1}
VIII	$K_2HPO_4•3H_2O$	131 mg L^{-1}	

The final pH should be 6.7-6.9.

493 Supplementary Table 16. Medium for *D. salina*.

Provasoli Stock Solution			
Component	**Element type**	**Initial concentration**	**End concentration**
I	$CaCl_2•2H_2O$	10 mg L^{-1}	/
II	$MgSO_4•7H_2O$	1230 mg L^{-1}	/
III	$NaNO_3$	420 mg L^{-1}	10-15 mg L^{-1}
	$NaH_2PO_4•2H_2O$	15.6 mg L^{-1}	0.01-0.02 mg L^{-1}
	$NaHCO_3$	840 mg L^{-1}	/
	KCl	74 mg L^{-1}	/
IV	$C_6H_8FeNO_7$	5 mg L^{-1}	/
V	NaCl	30 g L^{-1}	/
VI	H_3BO_3	2.86 mg L^{-1}	/
	$MnCl_2•4H_2O$	1.86 mg L^{-1}	/
	$ZnSO_4•7H_2O$	0.22 mg L^{-1}	/
	$Na_2MoO_4•2H_2O$	0.39 mg L^{-1}	/
	$CuSO_4•5H_2O$	0.08 mg L^{-1}	/
	$Co(NO_3)_2•6H_2O$	0.05 mg L^{-1}	/

494 The final pH should be 7.5.

Supplementary Table 17. Original carbonate system data (mean ± standard errors) determined from total alkalinity (TA) and pH at 6 °C, 32‰ salinity in the laboratory experiment using the CO2SYS Package.

Treatment	pH	CO_2 (ppm)	pCO_2 (μatm)	TA (μmol L^{-1})	DIC (μmol L^{-1})	CO_2 (μmol L^{-1})	CO_3^{2-} (μmol L^{-1})	HCO_3^- (μatm)
280	8.21 ± 0.07	291 ± 8	241 ± 54	2147 ± 91	1940 ± 108	12 ± 3	145 ± 16	1783 ± 116
400	8.13 ± 0.06	408 ± 8	272 ± 4	1937 ± 153	1779 ± 166	14 ± 3	110 ± 5	1655 ± 166
700	7.91 ± 0.06	703 ± 15	560 ± 102	2298 ± 93	2201 ± 108	29 ± 5	85 ± 7	2088 ± 110
1000	7.82 ± 0.02	1037 ± 35	789 ± 42	2622 ± 40	2548 ± 42	40 ± 2	80 ± 3	2428 ± 41
1500	7.67 ± 0.02	1520 ± 34	1153 ± 47	2644 ± 39	2621 ± 36	59 ± 2	58 ± 3	2504 ± 34
2000	7.51 ± 0.01	1960 ± 21	1733 ± 61	2694 ± 42	2723 ± 44	88 ± 3	42 ± 1	2593 ± 42

Supplementary Table 18. Original carbonate system data (mean ± standard errors) determined from total alkalinity (TA) and pH at 6 °C, 32‰ salinity in the laboratory experiment using the CO2SYS Package in CO_2/pH manipulation experiment.

Treatment	pH	CO_2 (ppm)	pCO_2 (μatm)	TA (μmol L^{-1})	DIC (μmol L^{-1})	CO_2 (μmol L^{-1})	CO_3^{2-} (μmol L^{-1})	HCO_3^- (μatm)
400+8.1	8.10 ± 0.01	404 ± 9	481 ± 26	3238 ± 134	3025 ± 130	25 ± 1	177 ± 6	2824 ± 123
400+7.8	7.81 ± 0.01	404 ± 9	486 ± 8	1578 ± 42	1524 ± 40	25 ± 0.4	46 ± 2	1452 ± 38
400+7.5	7.52 ± 0.02	404 ± 9	542 ± 17	874 ± 8	871 ± 6	28 ± 1	14 ± 1	830 ± 6
1000+8.1	8.11 ± 0.01	1025 ± 33	920 ± 9	6031 ± 23	5690 ± 19	47 ± 1	329 ± 4	5315 ± 17
2000+8.1	8.09±0.02	1981 ± 19	1683 ± 114	11467 ± 767	10842 ± 725	86 ± 6	650 ± 49	10106 ± 674

Supplementary Table 19. *C. reinhardtii* and *D. salina* culture conditions in natural seawater.

	Treatment	CO_2 (ppm)	pH
C. reinhardtii	**400 ppm**	404 ± 10	7.01 ± 0.01
	1000 ppm	1022 ± 30	6.92 ± 0.01
	2000 ppm	1978 ± 36	6.85 ± 0.01
D. salina	**400 ppm**	404 ± 10	8.22 ± 0.03
	1000 ppm	1022 ± 30	7.85 ± 0.02
	2000 ppm	1978 ± 36	7.51 ± 0.02

Supplementary Table 20. *C. reinhardtii* and *D. salina* culture conditions in artificial seawater.

	Treatment	CO_2 (ppm)	pH
C. reinhardtii	**400ppm+7.0**	408 ± 8	7.00 ± 0.01
	400ppm+6.9	408 ± 8	6.91 ± 0.01
	400ppm+6.8	408 ± 8	6.86 ± 0.01
	1000ppm+7.0	1020 ± 39	7.00 ± 0.01
	2000ppm+7.0	1971 ± 17	7.01 ±0.01
D. salina	**400ppm+8.2**	408 ± 8	8.24 ± 0.03
	400ppm+7.8	408 ± 8	7.82 ± 0.03
	400ppm+7.5	408 ± 8	7.51 ± 0.02
	1000ppm+8.2	1020 ± 39	8.21 ± 0.07
	2000ppm+8.2	1971 ± 17	8.21 ± 0.09

Supplementary Table 21. Photosynthesis vs light curve. P means photosynthesis, I means light.

CO_2 (ppm)	Equation	R^2
280	$P = -(6.04*10^{-8}*I + 7.14*10^{-7} - SQRT((6.04*10^{-8}*I + 7.14*10^{-7})* (6.04*10^{-8}*I + 7.14*10^{-7}) + 2.5*10^{-17}))/157446.3 -1.84*10^{-9}$	0.983
400	$P = (3.04*10^{-10}*I + 7.62*10^{-9} - SQRT((3.04*10^{-10}*I + 7.62*10^{-9})* (3.04*10^{-10}*I + 7.62*10^{-9}) - 1.11*10^{-26}))/1.652 -1.46*10^{-9}$	0.996
700	$P = (8.11*10^{-11}*I - SQRT((8.11*10^{-11}*I)* (8.11*10^{-11}*I))) +0.001*10^{-9}$	0.781
1000	$P = (3.53*10^{-10}*I + 1.01*10^{-8} - SQRT((3.53*10^{-10}*I + 1.01*10^{-8})* (3.53*10^{-10}*I + 1.01*10^{-8}) - 1.59*10^{-26}))/1.822 -1.22*10^{-9}$	0.998
1500	$P = (3.10*10^{-10}*I + 7.88*10^{-9} - SQRT((3.10*10^{-10}*I + 7.88*10^{-9})* (3.10*10^{-10}*I + 7.88*10^{-9}) -7.23*10^{-27}))/1.558 -9.5*10^{-10}$	0.998
2000	$P = (2.12*10^{-10}*I - 5.31*10^{-9} - SQRT((2.12*10^{-10}*I - 5.31*10^{-9})* (2.12*10^{-10}*I - 5.31*10^{-9}) - 2.27*10^{-26}))/0.794 +1.27*10^{-8}$	0.983